Computer Modelling in Ocean Engineering 91, Arcilla et al. (eds) © 1991 Balkema, Rotterdam. ISBN 90 5410 024 9

Application of computer graphics on water wave problems

S.S.Hsiao & C.R.Chou
National Taiwan Ocean University, Department of River & Harbour Engineering, Taiwan

ABSTRACT: To make water wave graphs more realistic in vision, and to display the process of wave transformation more clearly, a computer graphic software is applied to paint water wave profiles in color. As demonstration, two cases were studied in this paper: wave evolution around cylinder and in harbor basin, both having arbitrary shapes. Surface elevations were calculated using boundary element method. Calculated results were then transformed into 3-D color graphs, to be displayed on monitor by the software. Finally, animation frames of wave evolution was presented by applying assembly programs to control the storage and display of graphic images for each time step. It is concluded that, satisfactory results could be achieved through this procedure.

1 INTRODUCTION

By studying water wave problems numerically, calculated results were often presented collectively in graphs. For example, to describe changes of wave forms due to presence of off-shore structures, or modifications of surface elevations arounsed by harbour resonance, wave contours were plotted in one (or a series of) diagram(s). However, it would seem to be rather unrealistic to exemplify characteristics of a three dimensional water wave problem just on plane figures. Recently, significant progress in computer graphic has been made, which enable us to plot wire frame graphs of 3-D wave profiles, i.e., to express a 3-D object through 2-D graphs. Nevertheless, wire-frame graphs are still, more or less, unrealistic in vision. In this paper, a computer graphic software was applied to paint water wave profiles in color. A brightening procedure was then used in accordance with the origin of a light source. In this way, water wave graphs could be presented more realistically in vision.

Two cases were considered in this paper: wave evolution around cylinder and in harbor basin, both having arbitrary shapes. Since neither surface elevations near the boundary of the structures, nor animation frames of wave evolution can be calculated using this software, computer programs were developed to handle thses problems. Solutions of surface elevations were obtained applying numberical models developed by Chou (Chou, 1983; Chou & Yeh, 1981; Chou & Lin, 1985). A dimensionless wave period, $\sigma^2 h/g$, was chosen as reference parameter, σ is the angular frequency of these waves, g is the gravitational acceleration, and h is water depth. For circular-, as well as elliptic-shaped cylinders, this dimensionless parameter was chosen to be 0.5. For harbour basins having circular and rectangular shape, it has a value of 1.2. Calculated wave profiles were transformed into 3-D color graphs and displayed dynamically on a color monitor.

2 DESCRIPTION AND AUGMENTATION OF THE SOFTWARE

2.1 Description

The computer graphic software, MORE, was developed by the Ota et al. (Ota et al., 1986). It was used to manipulate the removal of hidden surface, as well as to paint wave profiles in color. The MORE graphic system is composed of four subsystems: Modeling, Motion-Design, Rendering and Recording (Fig. 2-1). Only the first and the third subsystems were used in this paper.

A short description of these two subsystems might be in place:

1 The Modeling Subsystem
The geometric data of the object under consideration will be stored in a model file. Parameters concerning view volume, light source and brightness will be kept in a parameter file. Then, applying the Modeling subsystem, these two files can be combined to yield a polygon file which can plot wire-frame graphs on monitor.

2 The Rendering subsystem
The Rendering subsystem consists of two programs: render.c and dither.c. When the render.c program is executed, it will read the polygon file from the modeling subsystem at first, and then after removing the hidden-surfaces, painting the graphs in color, and applying the brightening procedure, an image file will be created. This image file will be transformed into 3-D color graphs on the monitor by the dither.c program.

2.2 Augmentation

Before using the modeling subsystem, data of the curved surface must be found in the first place. Since, as mentioned earlier, this graphic softward can neither calculate wave profile, nor can it make animation frames, supplemental programs were designed to meet these requirements. These four programs are:

1 Transformation of the surface profile
Calculated surface profile will be rearranged in order to match the reading format of the graphic software.

2 Plotting the graphs of the structure
Polygon meshes of the curved surface is combined to approximate the 3-D shapes of the structure. In general, the cross-section of the structure is divided into N nodes. These were then connected yielding a polygon. Better approximation can be achieved when the number of the nodes is large enough and the nodes are distributed smoothly. For example, the cross-sections of a vertical cylinder were plotted first, then two nodes on the top cross-section and two on the bottom were chosen. A rectangular mesh can be acquired by connecting these nodes. In this way, the shape of the vertical cylinder can be represented by combining a number of these rectangular meshes. A circular cylinder represented by rectangular meshes is shown in Figure 2-2. The data concerning the shapes of the structure were saved in a model file which is used as input data of the Modeling subsystem.

3 Calculating the boundary of the curved surface
Curved surface of the water wave profile was calculated by the bi-cubic B-spline method in this paper. In order to make the surface more continuously and more smoothly, 16 points were chosen as control points to determine the surface mesh at the center (see Figure 2-3). However, meshes of the curved surface in the vicinity of the structure can not be obtained through this procedure. To demonstrate this, surface meshes around a circular cylinder will be considered. Figure 2-4 shows the divided regions around a circular cylinder where the intersection points are control points. Polygon meshes of the curved surface obtained by calculating the control points are shown in Figure 2-5. Clearly, curved surface meshes near the boundary of the cylinder were not obtained. These polygon meshes were determined in the following way: the edge points of the curved surface facing the boundary of cylinder were first taken to match with the nodal points on the boundary. Then, every 4 neighboring points were connected to construct a polygon mesh near the boundary of cylinder (see Figure 2-6). Finally, these two parts of the polygon mesh data were combined to create a polygon file of the water surface profile to be used in the Modeling subsystem.

4 Animation
To display the simulated process of wave evolution continuously, a Store-Display subsystem was developed. This sub-system is consisted of two parts. The first part stores color graphs of the wave profile in computer memory for each time step. The second part controls the continuous display of the stored color graphs on the monitor screen.

3 3-D GRAPHS OF WATER WAVE PROFILE

3.1 Curved surface meshes of the wave profile

Boundary element method was used to obtain the numerical results of water surface elevation. The region of interest was divided into rectangular meshes. Then, using the coordinates of their intersection points together with the dimensionless wave period, $\sigma^2 h/g$, as input, surface elevation at every mesh point could be found. The coordinates of the 16 neighboring mesh points were then taken as control points for the bi-cubic B-spline method. Combining

every 16 neighboring points in the region, a data file of the control points (named *.ctl) could then established.

Except for regions in the vicinity of the structure, polygon meshes of the water wave profiles in the region of interest can be obtained through this data file and the B-spline method. The polygon meshes near the boundary of the structure can be obtained through the procedure mentioned in section 2.2. Finally, a polygon mesh data file (named *.pol) of water wave profile is created by combining all the polygon meshes.

3.2 3-D graphs of the wave profile

By putting the model file of the structure and the polygon mesh data file of the wave profile into the Modeling subsystem, wire-frame graphs of water waves around structure are ready to be displayed on a monitor. To make the graphics more vividly, parameters like view volume, color, brightness etc. must be taken into consideration. These control parameters were written in a a model file (named *.mod). Through the Modeling subsystem, the polygon file (*.pol) and the model file (*.mod) were then combined to become an input data file for the Rendering subsystem. When executing the render.c and dither.c programs, 3-D color graphs of water waves would be displayed on a monitor. According to the quality of the visual effects, the parameters in the parameter model file were revised many times until optimum graphs were found.

3.3 Presenting animation frames

Since progressive waves under consideration are both time-depend and periodic, the wave period is discretized into 24 time steps. Water wave profiles were calculated for each time step to be presented on the monitor. Simulation of the actual wave evolution process requires that wave profiles to be presented in time series. This requirement is fulfilled by applying the Store-Display subsystem, which controls the storage of water wave graphs according to the time steps and their display.

Besides being more realistic, it seem that, the process of wave transformation could be demonstrated more clearly through this procedure. The flow chart for presenting the animation frames of water waves is shown in figure 3-1.

4 FORMULATION OF RELATIVE WATER WAVE PROBLEMS

Under the assumption of ideal, incompresible fluid and irrotational flow, motion of small amplitude waves in water of constant depth can be described by a velocity potential Φ. In the following the usual notations are used, with g the gravitational acceleration, ζ_0 the amplitude, σ the wave frequency, and $\phi(x,y,z)$ is the potential function, t is time and $i = \sqrt{-1}$, the imaginary constant. The potential function $\phi(x,y,z)$ is governed by the Laplace equation:

$$\partial^2 \phi / \partial x^2 + \partial^2 \phi / \partial y^2 + \partial^2 \phi / \partial z^2 = 0 \quad (4\text{-}1)$$

4.1 Surface elevation around vertical cylinder

A large vertical cylinder of arbitrary cross section is assumed to exit in waters of constant depth h. One end of the cylinder is mounted on the sea bottom with the other end piercing out of the free surface. A Cartesian coordinate system oxyz is defined with the origin on the undisturbed free surface and the oz axis pointing vertically upwards (Figure 4-1).

The boundary condition of the free surface and the impermeable sea bottom are specified as follow:

$$\left.\begin{array}{ll} \partial \phi / \partial z = \sigma^2 / g \cdot \phi & , z = 0 \\ \partial \phi / \partial z = 0 & , z = -h \end{array}\right\} \quad (4\text{-}2)$$

Hence the solution of $\phi(x,y,z)$ that satisfies equation (4-1) can be expressed as:

$$\phi(x,y,z) = [\, f_0(x,y) + f^*(x,y) \,] \cdot \cosh k(z+h) / \cosh kh \quad (4\text{-}3)$$

where $f_0(x,y)$ and $f^*(x,y)$ are the incident and diffracted waves, respectively. k denotes the wave number of the incident wave and is given by dispersion relation:

$$kh \cdot \tanh kh = \sigma^2 h / g \quad (4\text{-}4)$$

If ω represents the angle between the direction of wave propagation and the ox axis, then the surface profile of the incident wave can be described by:

$$\zeta_i(x,y;t) = \zeta_0 \cdot \cos[\, k(x\cos\omega + y\sin\omega) + \sigma t \,] \quad (4\text{-}5)$$

And the incident wave $f_0(x,y)$ is given by:

$$f_0(x,y) = -i \exp[\, -ik(x\cos\omega + y\sin\omega) \,] \quad (4\text{-}6)$$

Substituting Equation (4-3) into the Laplace equation, Equation (4-1), it is clear that f*(x,y) should satisfy the two-dimensional Helmholtz equation:

$$\partial^2 f^*/\partial x^2 + \partial^2 f^*/\partial y^2 + k^2 f^* = 0 \qquad (4\text{-}7)$$

Since the structure is impermeable, the normal velocity on it should be zero. Thus:

$$\partial\phi/\partial n = 0 \qquad (4\text{-}8)$$

where $\partial\phi/\partial n$ is the normal derivative on the surface. Substituting Equation (4-3) into Equation (4-8), the relation between f_0 and f* on the cylinder surface is found to be:

$$\partial f_0/\partial n = -\partial f^*/\partial n \qquad (4\text{-}9)$$

Using these formulae and applying the numerical model developed by Chou (1983, Chou & Yeh, 1981), the function f*(x,y) in the domain of interest can be found. Substituting of f*(x,y) into Equation (4-3), the velocity potential $\phi(x,y,z)$ can be obtained. According to the Airy wave theory, the surface profile of water waves can be expressed as:

$$\zeta(x,y;t) = i\zeta_0\phi(x,y,0)\exp(-i\sigma t) \qquad (4\text{-}10)$$

Substituting the value of $\phi(x,y,0)$ into Equation (4-10), one may obtain surface elevation in the domain of interest.

4.2 Analysis of the harbor resonance

A harbour basin of arbitrary shape with water of constant depth h is shown in Figure 4-2. The domain of interest was divided into three regions: an open-sea region and two harbour regions. The coastlines AB, EF are assumed to be nature beaches, and can absorb wave energy completely. Other boundaries are assumed to be impermeable. The potential function for every region can be written as:

$$\phi_1(x,y,z) = [f_0(x,y) + f_1(x,y)]\frac{\cosh k(z+h)}{\cosh kh}$$

$$\phi_2(x,y,z) = f_2(x,y)\frac{\cosh k(z+h)}{\cosh kh}$$

$$\phi_3(x,y,z) = f_3(x,y)\frac{\cosh k(z+h)}{\cosh kh} \qquad (4\text{-}11)$$

where f_0 and f_1 are incident and reflected waves in the open sea region, f_i (i=2,3) represent diffracted waves within the harbour region I and II.

The function $f_0(x,y)$ of the incident wave is specified as:

$$f_0(x,y) = -i\exp[-ik(x\cos\omega + y\sin\omega)] \qquad (4\text{-}12)$$

According to Eq.(4-1), f_i (i=1,2,3) should satisfy the following Helmholtz equation:

$$\partial^2 f_i/\partial x^2 + \partial^2 f_i/\partial y^2 + k^2 f_i = 0 \qquad (4\text{-}13)$$

Besides the free surface and the impermeable bottom floor conditions, other relevant boundary conditions are:

1) The velocity normal to the impermeable boundaries are zero:

$$\partial\phi_i/\partial n = 0 \qquad i = 1,2,3 \qquad (4\text{-}14)$$

2) For the imaginary boundary B_1 between regions of the open sea and the harbor I, the mass and energy fluxes of the fluid must be continuous:

$$\left.\begin{aligned}\partial\phi_1/\partial n &= \partial\phi_2/\partial n\\ \phi_1 &= \phi_2\end{aligned}\right\} \qquad (4\text{-}15)$$

3) The same continuity conditions must also hold for the imaginary boundary B_2 between regions within the harbor, i.e., I and II:

$$\left.\begin{aligned}\partial\phi_2/\partial n &= \partial\phi_3/\partial n\\ \phi_2 &= \phi_3\end{aligned}\right\} \qquad (4\text{-}16)$$

Applying the numerical methods described by Chou (1983; Chou & Lin, 1985), the velocity potential $\phi(x,y,z)$ can be obtained. Surface elevations within the harbour area can then be acquired according to Eq. (4-10).

5 APPLICATION AND CONCLUSION

Surface elevations aroused by waves due to the presence of cylinder and harbor are studied in this paper. For the cases of cylinders, a dimensionless period $\sigma^2 h/g$ = 0.5 is chosen. Cases studied are: circular cylinder with a radious of 1.6h, where h is the water depth; elliptically shaped cylinder having a long axis of 1.6h and a short axis of 0.8h. As for the cases of harbors, a dimensionless period of $\sigma^2 h/g$ = 1.2 is selected for both a rectangular harbor with a width of 10h and a length of 20h, as well as a circular shaped basin having an entrance of 5h with a radius of 5h. Wave periods are divided into 24 discrete time steps and surface elevations are calculated and plotted accordingly.

Wave evolutions are hard-copied directly from the monitor using a NEC PR-801 color printer. Figs. 5-1 to 5-4 are for the cylinder cases with $\sigma^2 h/g$ = 0.5, $\sigma t = 0^\circ$, 30° of circular and elliptical shape. Figs. 5-5 to 5-8 are for harbor basins with $\sigma^2 h/g$ = 1.2, $\sigma t = 0^\circ$, 30° with rectangular and circular shapes.

Results of this study indicate that, when water waves were obstructed by structure or harbour oscillation, the time history of wave transformation could be clearly visualized through the procedure proposed here in this paper. It seems advisable to express wave evolution process this way, since a more vivid picture could be presented. We have studied regular waves only in this paper, however, it would be interesting to exemplify other cases, e.g., short-crested waves, in a similar way.

REFERENCES

Chou, C.R. & R.C. Yeh 1981. Nonlinear wave forces on offshore structure. J. Chinese Inst. Civil & Hydraulic Engng. vol. 7(4) pp.53-61 (in Chinese)

Chou, C.R. 1983. Application of boundary element method on water wave problems. Rep. Dept. River & Harbor Engng. National Taiwan Ocean Univ. Keelung, Taiwan pp.227 (in Chinese)

Chou, C.R. & J. G. Lin 1985. Numerical analysis of harbor oscillation with arbitrary shape and depth. Proc. 8th Conf. Ocean Engng. Rep. China October, pp.111-129 (in Chinese)

Ota, M., A. Takeuchi & T. Oguchi 1986. Applied Graphics. ASCII Company, Tokyo, Japan (in Japanese)

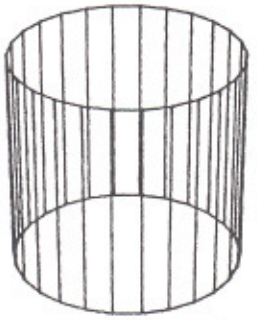

Fig. 2-2 A circular cylinder decomposed into rectangular meshes

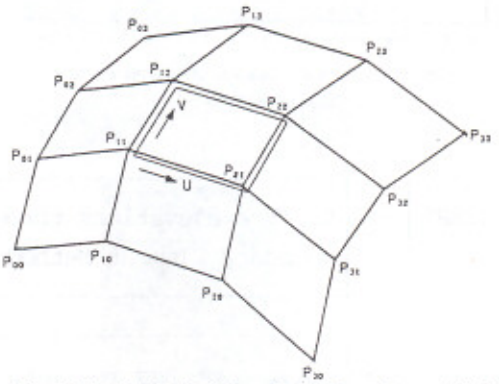

Fig. 2-3 Control points of the B-spline method

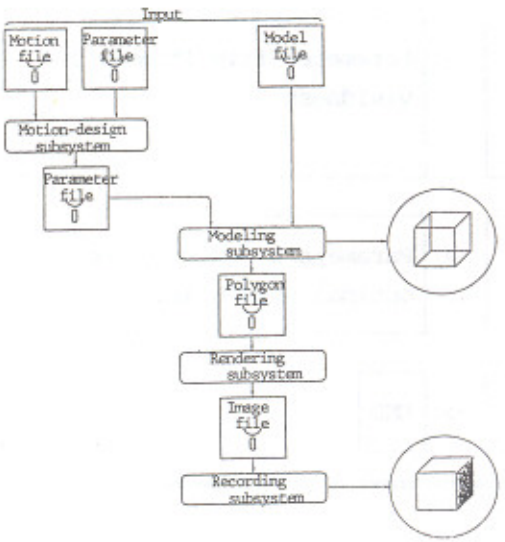

Fig. 2-1 Overview of the MORE System

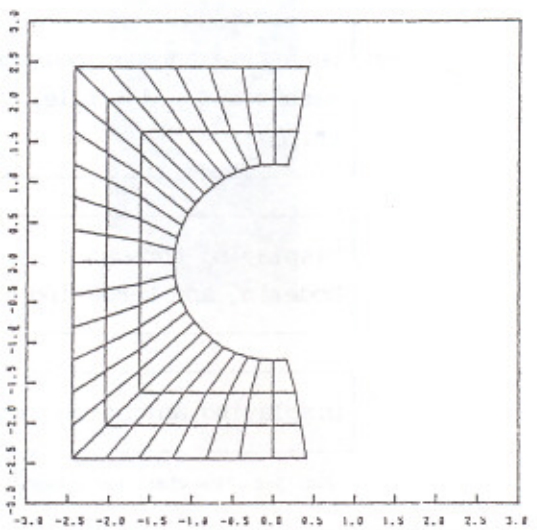

Fig. 2-4 Discretized regions around a circular cylinder

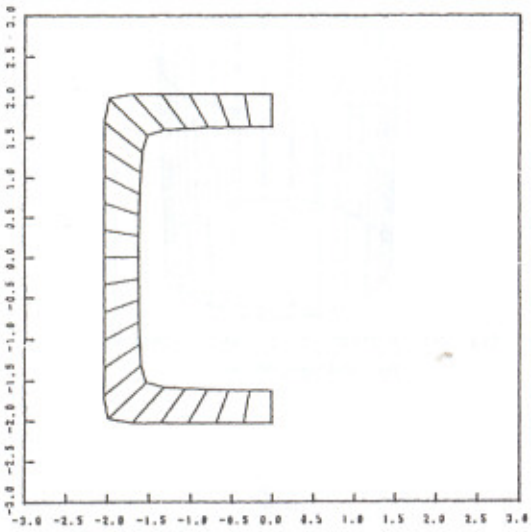

Fig. 2-5 Polygon meshes obtained by the B-spline method

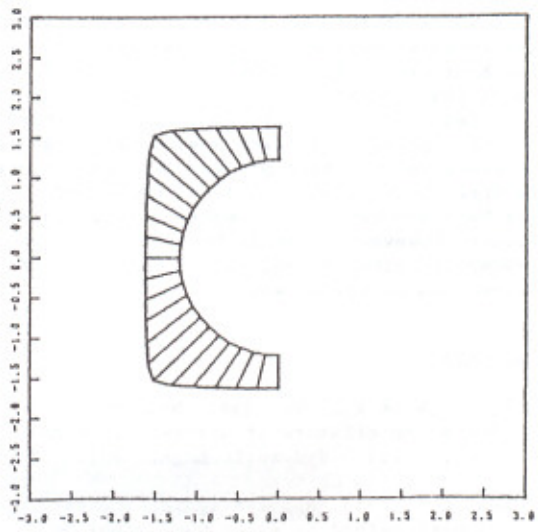

Fig. 2-6 Polygon meshes near the boundary of the cylinder

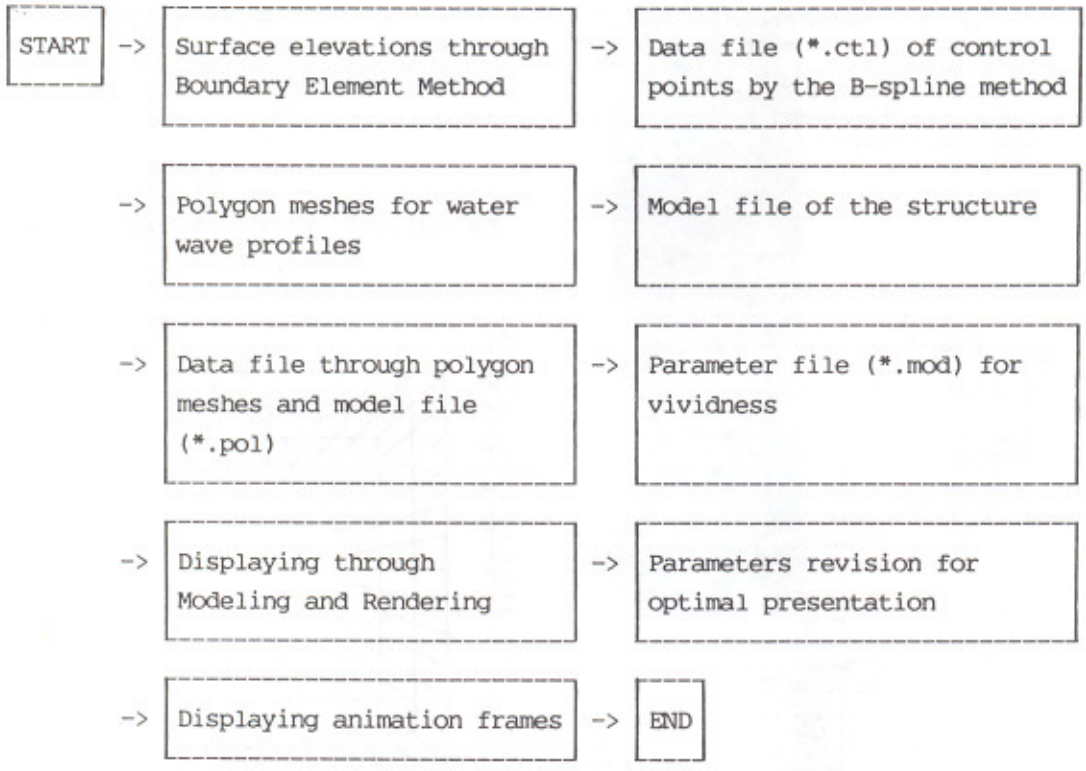

Fig. 3-1 Flow chart for presenting animation frames of the water waves

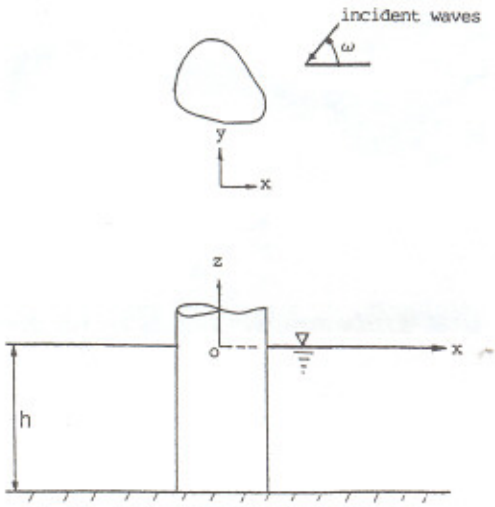

Fig. 4-1 Definition sketch for vertical cylinder

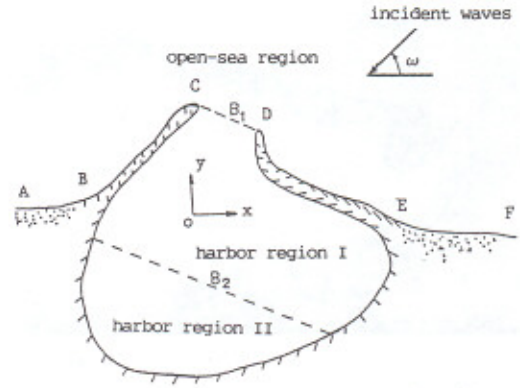

Fig. 4-2 Definition sketch for an arbitrarily shaped harbor

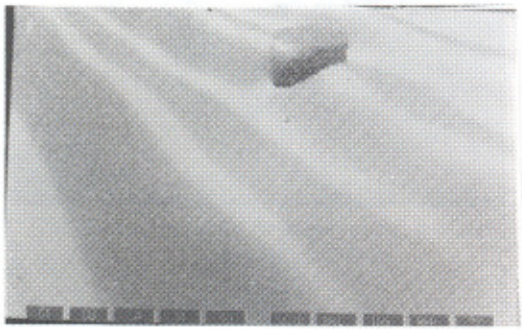

Fig. 5-1 Water waves around circular cylinder $\sigma^2 h/g=0.5$, $\sigma t=0^\circ$

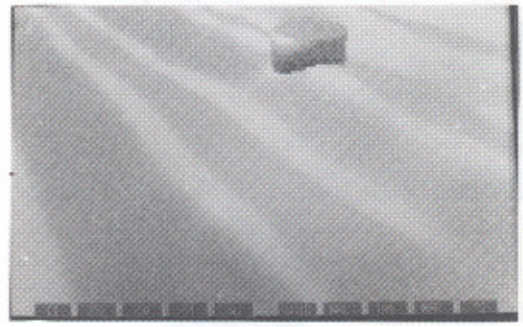

Fig. 5-2 Water waves around circular cylinder $\sigma^2 h/g=0.5$, $\sigma t=30^\circ$

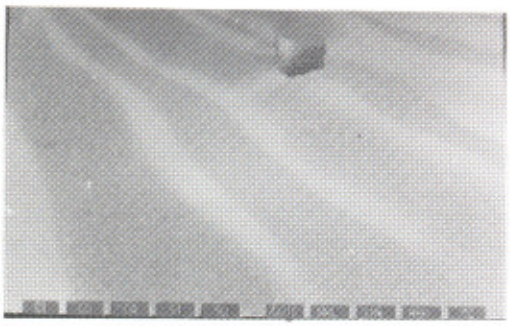

Fig. 5-3 Water waves around elliptic cylinder $\sigma^2 h/g=0.5$, $\sigma t=0^\circ$

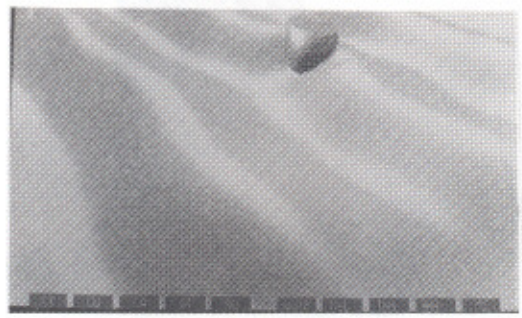

Fig. 5-4 Water waves around elliptic cylinder $\sigma^2 h/g=0.5$, $\sigma t=30^\circ$

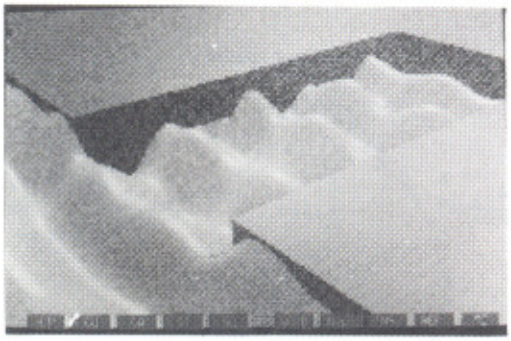

Fig. 5-5 Water waves in rectangular harbour
$\sigma^2 h/g=1.2$, $\sigma t=0°$

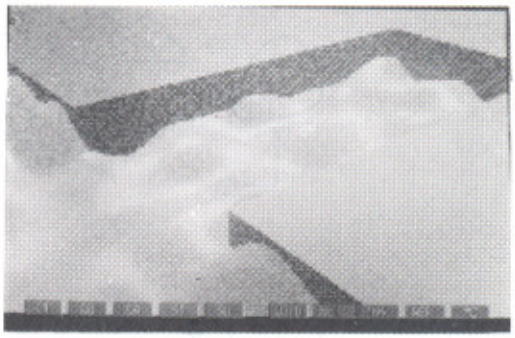

Fig. 5-6 Water waves in rectangular harbour
$\sigma^2 h/g=1.2$, $\sigma t=30°$

Fig. 5-7 Water waves in circular harbour
$\sigma^2 h/g=1.2$, $\sigma t=0°$

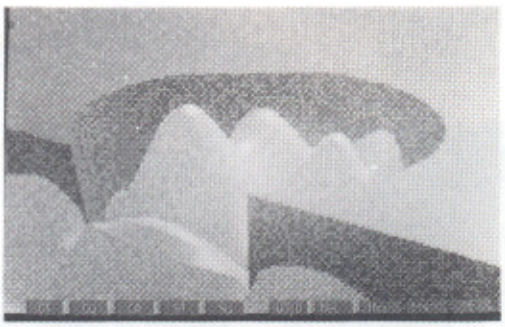

Fig. 5-8 Water waves in circular harbour
$\sigma^2 h/g=1.2$, $\sigma t=30°$